Ab Initio Study of 2,4-Substituted Azolidines. II. Amino−Imino Tautomerism of 2-Aminothiazolidine-4-one and 4-Aminothiazolidine-2-one in Water Solution

Venelin Enchev,* Nadezhda Markova, and Silvia Angelova

Institute of Organic Chemistry, Bulgarian Academy of Sciences, 1113 Sofia, Bulgaria

Received: May 16, 2005; In Final Form: July 29, 2005

The relative stabilities of the tautomers of 2-aminothiazolidine-4-one and 4-aminothiazolidine-2-one were calculated at the MP2/6-31+G(d,p) level by considering their mono- and trihydrated complexes. Single-point calculations at the MP4/6-31+G(d,p)//MP2/6-31+G(d,p) level of theory were performed to obtain more accurate energies. The values of proton transfer barriers in the isolated, mono- and trihydrated tautomers of 2-aminothiazolidine-4-one (2AT) and 4-aminothiazolidine-2-one (4AT) were calculated for two different mechanisms of tautomerisation. In the absence of water, the process of proton transfer should not occur. Addition of water molecules decreases the barrier making the process faster, as the participation of two water molecules in a proton transfer reaction is more favorable than the participation of only one water molecule. To estimate the effect of the medium (water) on the relative stabilities of the tautomers of the studied compounds we applied the polarizable continuum model (PCM). ^{13}C NMR chemical shieldings were calculated using the GIAO approach at MP2/6-31+G(d,p) optimized geometries. HF and the DFT B3LYP functional with 6-31+G-(d,p) basis set were employed. The quantum chemical results for the chemical shifts in gas phase and in polar solvents (water and DMSO) were compared with experimental data. TD DFT B3LYP/aug-cc-pVTZ calculations were performed to predict the absorption maxima of tautomers **A** and **B** of 2AT and 4AT.

1. Introduction

Solvation plays an important role among a number of physical and chemical factors responsible for equilibrium between tautomers. Studying the effects of solvation is important because the structure and reactivity of free molecules are very different from that in the solvent environment. Such a task is quite difficult because of the necessity of detailed examination of the interactions between the solute and the solvent molecules.

To simulate the solvent effect, two different methods can be used: the first takes into account the dielectric effect via the self-consistent reaction field (SCRF), the second is the super-molecule approach that considers explicitly the formation of solute−water complexes. The latter model is appropriate for studying the dynamics of proton-transfer reactions. In this case explicit interaction with a limited number of water molecules could influence the reaction path by lowering the potential energy barrier due to their direct participation in proton transfer. A combined approach (SCRF + supermolecule) could also be used.

Recently, we studied the amino−imino tautomerism of 2-aminothiazolidine-4-one (pseudothiohydantoin, 2AT) and 4-aminothiazolidine-2-one (4AT) in weakly polar ($CHCl_3$) and polar (DMSO) solvents.[1] In the present work, 2AT and 4AT are investigated aiming to understand their behavior in protic solvents.

Experimental studies on the amino-imino tautomerism of 2-aminothiazolidine-4-one have been reported in several papers.[2−14] However, the opinions of the authors are contradictory. Amirthalingam and Muralidharan[7] have confirmed by X-ray the existence of the imino form of pseudothiohydantoin. Twenty-two years later Steel and Guard[14] have redetermined the crystal structure of pseudothiohydantoin at 128 K and have shown that the compound exists in the amino form. Using UV−vis spectral data, Comrie[3] and Akerblom[4] have reported that in water solution both tautomeric forms exist with domination of the imino tautomer. By means of IR spectroscopy, Khovratovich and Chizhevskaya[5] have shown that in chloroform solution the amino form exists. According to Ramsh et al.[11] (IR and NMR data), in DMSO and in water solutions pseudothiohydantoin exists as amino tautomer. Studies[13] of 2-aminothiazolidine-4-one and its isomer 4-aminothiazolidine-2-one have been carried out by IR and ^1H and ^{13}C NMR spectroscopy in DMSO solution and have shown that 2AT exists in amino form while 4AT in imino form.

Proton transfer can be viewed as the simplest model of a tautomerization reaction. To model the proton transfer in 2AT and 4AT by the supermolecule approach, one should add one or more water molecules to the solute. We will try to answer the following questions: How does the water medium affect the relative stabilities of the amino and imino tautomers of 2AT and 4AT? What role do the water molecules play in the tautomerism process? The present work gives results for the geometries and energetics of the complexes of 2AT and 4AT with one and three water molecules and compares two possible mechanisms of proton transfer.

2. Computational Details

Ab initio calculations using many-body perturbation theory (MBPT) were carried out for the study of the interaction of solute tautomers with one or three water molecules. All geometries of the minima and the transition structures for tautomeric conversions were located at MP2/6-31+G(d,p) level without symmetry restrictions by the gradient procedure.

* Corresponding author. E-mail: venelin@orgchm.bas.bg. Fax: ++359 2 8700225.

10.1021/jp052560w CCC: $30.25
Published on Web 09/10/2005

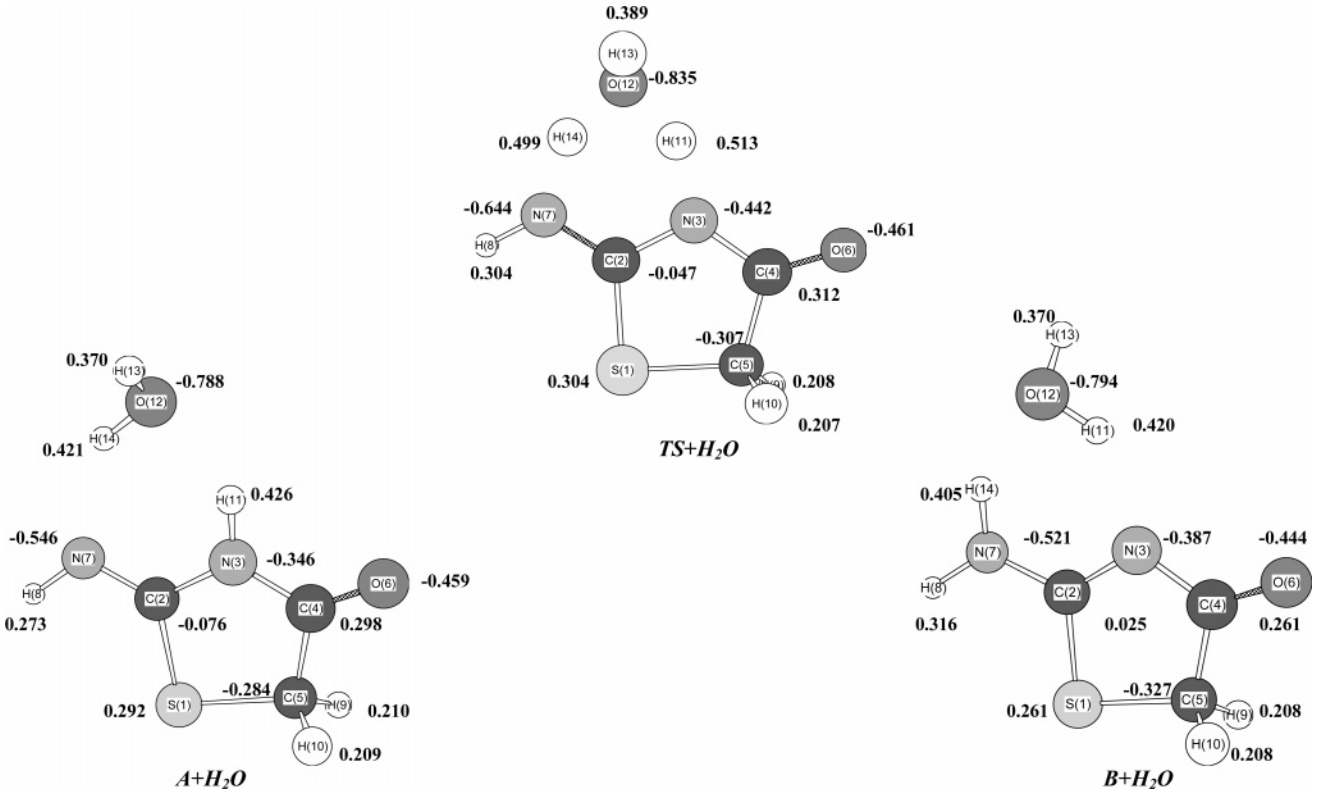

Figure 1. Monohydrated complexes of 2AT optimized at MP2/6-31+G(d,p) level. Mulliken charges (e^-) on the atoms are given.

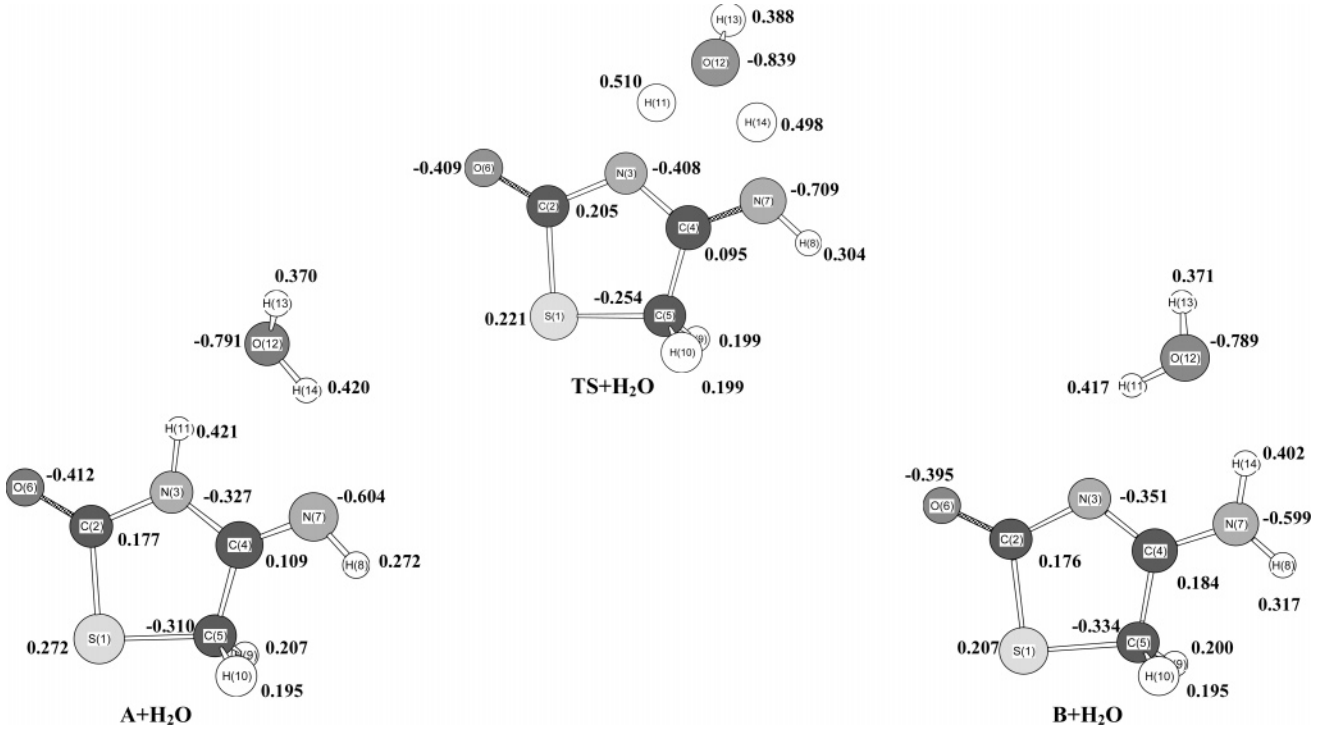

Figure 2. Monohydrated complexes of 4AT optimized at MP2/6-31+G(d,p) level. Mulliken charges (e^-) on the atoms are given.

Frequency calculations at the same level of theory were carried out for all the complexes reported in the study to determine whether the optimized structures are local minima or transition states (TS) and to estimate thermal corrections to 298.15 K.

Single-point calculations at MP4/6-31+G(d,p)//MP2/6-31+G-(d,p) level of theory were performed to obtain more accurate energies. MP2/6-31+G(d,p) zero point energies (ZPE) were added to the total energies. The values of Gibbs free energies (ΔG) and the populations (p_i) were calculated by the standard formulas $\Delta G = \Delta H - T\Delta S$ and

$$p_i = e^{-\Delta G_i/RT} / \sum_i e^{-\Delta G_i/RT}$$

respectively. To estimate ΔH values, thermal corrections to the enthalpies calculated at MP2/6-31+G(d,p) level were added to the calculated energies. The entropy values were evaluated from the frequency calculations at the level of optimization. The

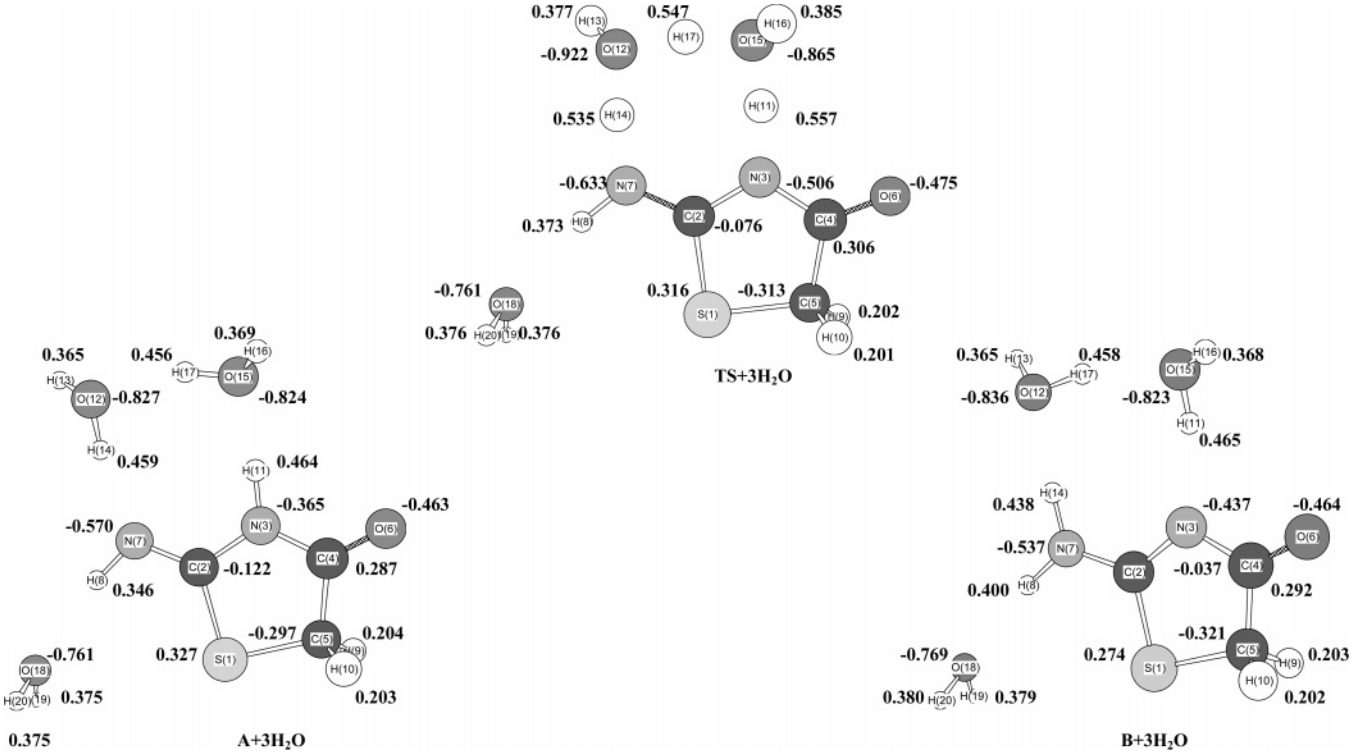

Figure 3. Trihydrated complexes of 2AT optimized at MP2/6-31+G(d,p) level. Mulliken charges (e^-) on the atoms are given.

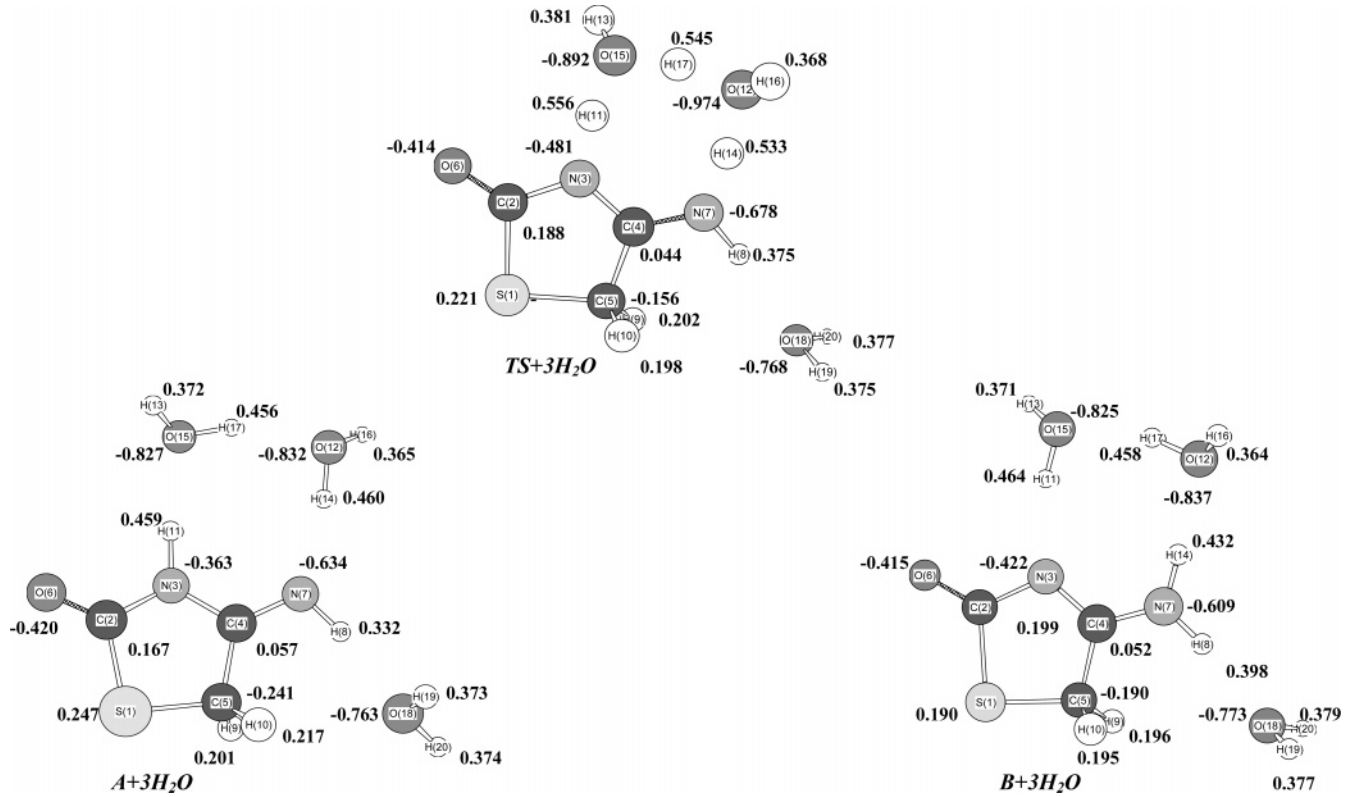

Figure 4. Trihydrated complexes of 4AT optimized at MP2/6-31+G(d,p) level. Mulliken charges (e^-) on the atoms are given.

classical rate constant at 298.15 K was calculated using the Eyring equation, $k = k_B(T/h)e^{-\Delta G^{\#}/RT}$, where k_B and h are the Boltzmann and Planck constants, respectively.

To establish the connection between the transition structure and the corresponding equilibrium structures in the trihydrated complex of the solute, the reaction pathway was followed using the intrinsic reaction coordinate (IRC) procedure. The fourth-order Runge−Kutta (RK4) algorithm[15,16] implemented in the GAMESS program package was used to obtain the IRC of the water-mediated PT reaction. The reaction path was followed from the transition state to the reactant and to the product using a step size of 0.05 $au^{1/2}$ bohr.

The calculations were carried out using the PC GAMESS version[17] of the GAMESS (US) quantum chemistry package.[18]

To estimate the effect of the medium (water) on the relative stabilities of the tautomers of the studied compounds we applied

TABLE 1: MP2/6-31+G(d,p) and MP4/6-31+G(d,p)//MP2/6-31+G(d,p) Calculated E_T, ZPE (a.u.), and ΔE_T (kcal mol^{-1})

	MP2/6-31+G(d,p)			MP4/6-31+G(d,p)//MP2/6-31+G(d,p)	
species	E_T	ΔE_T	ZPE	E_T	ΔE_T
		2AT			
A	−698.272158	0.00	0.077937	−698.308887	0.00
B	−698.271826	0.21	0.077647	−698.306565	1.45
$TS_{(A\rightarrow B)}$	−698.193907	49.10	0.071668	−698.223668	53.48
A + H_2O	−774.523468	0.84	0.103204	−774.566497	0.00
B + H_2O	−774.524806	0.00	0.103049	−774.566215	0.18
$TS_{(A\rightarrow B)}$ + H_2O	−774.493811	19.45	0.096563	−774.529727	23.07
A + $3H_2O$	−927.019280	3.74	0.152752	−927.075705	2.85
B + $3H_2O$	−927.025240	0.00	0.152909	−927.080254	0.00
$TS_{(A\rightarrow B)}$ + $3H_2O$	−926.994408	19.35	0.143805	−927.042745	23.54
		4AT			
A	−698.273351	1.05	0.078268	−698.310178	0.00
B	−698.275037	0.00	0.077836	−698.309997	0.11
$TS_{(A\rightarrow B)}$	−698.194344	50.64	0.072288	−698.224243	53.93
A+H_2O	−774.524383	2.16	0.103044	−774.567424	1.26
B + H_2O	−774.527824	0.00	0.103392	−774.569426	0.00
$TS_{(A\rightarrow B)}$ + H_2O	−774.495110	20.52	0.096708	−774.531128	24.03
A + $3H_2O$	−927.021289	4.74	0.153600	−927.077653	4.03
B + $3H_2O$	−927.028838	0.00	0.153315	−927.084080	0.00
$TS_{(A\rightarrow B)}$ + $3H_2O$	−926.996856	20.07	0.144104	−927.045690	24.09

the polarizable continuum model (PCM)[19,20] as implemented in the GAUSSIAN 98[21] suite of programs at MP2/6-31+G(d,p) level for the geometries optimized at the same level of theory, i.e., PCM/MP2/6-31+G(d,p)//MP2/6-31+G(d,p).

^{13}C NMR chemical shieldings were calculated using the GIAO (gauge-including atomic orbitals) approach.[22,23] Chemical shieldings were calculated at MP2/6-31+G(d,p) optimized geometries. HF and the DFT B3LYP functional with 6-31+G(d,p) basis set were employed. To compare with experiment the calculated absolute shieldings were transformed to chemical shifts using the reference compound tetramethylsilane (TMS): $\delta = \delta_{calc}(TMS) - \delta_{calc}$. Both $\delta_{calc}(TMS)$ and δ_{calc} were evaluated with the same method and basis set.

The including of the solvent as dielectric (polarizable continuum model) in GIAO ^{13}C NMR calculations was used to estimate the effect of the medium (DMSO in the case of isolated species and water for complexes) on the chemical shifts of the more stable tautomers of the studied compounds. All NMR calculations were carried out using Gaussian 03.[24]

The MP2/6-31+G(d,p) optimized tautomer geometries were used for the vertical transition energy calculations in the time-dependent density functional theory (TDDFT)[25] employing the aug-cc-pVTZ basis set. The B3LYP functional was used in the TDDFT calculations.

3. Experimental Section

The 2-aminothiazolidine-4-one was synthesized according to Davies et al.[26] and the 4-aminothiazolidine-2-one was prepared according to Komaritsa.[27]

The NMR spectra were recorded on a Bruker DRX-250 spectrometer, operating at 250.13 MHz for ^{1}H and 62.9 MHz for ^{13}C, using a 5 mm dual ^{1}H/^{13}C probe head. For both compounds the power gated decoupling technique was used to obtain decoupled ^{13}C NMR spectra with signals enhanced by the NOE. The digital resolution for the decoupled ^{13}C spectra was 0.66 Hz/pt. Exponential multiplication with a line broadening factor of 1 Hz was applied to the FID in order to reduce the noise level. The NMR spectra in water and DMSO were calibrated relative to TMS used as an internal standard. The NMR spectra in water−methanol 1:1 mixture were calibrated relative to the signal of methanol.

The absorption spectra were scanned on a Shimadzu UV-mini 1240 UV−vis spectrophotometer. The measurements were performed of freshly prepared solutions with concentrations of 5×10^{-4} M L^{-1} for 2-aminothiazolidine-4-one and of 1.22×10^{-3} M L^{-1} for 4-aminothiazolidine-2-one. The molar extinction coefficients (ϵ) of 2AT and 4AT in water were examined.

4. Results and Discussion

In our previous paper,[1] we studied the relative stabilities of all tautomers of 2AT and 4AT. We showed that tautomers **A** and **B**, presented in Figures 1−4, are near in energy in the gas phase and in weakly polar ($CHCl_3$) and polar (DMSO) solutions. The amino tautomer **B** is more stable for both compounds.

4.1. Relative Stabilities in Water Solution. The effect of aqueous hydration is simulated using the supermolecule approach in which one or three water molecules are attached to the imino **A** and amino **B** tautomers. Water molecules are located in the appropriate positions to facilitate intramolecular proton transfer. The relative total energies of **A** and **B** of 2AT and 4AT and their mono- and trihydrated complexes are presented in Table 1.

In the monohydrated complexes of 2AT and 4AT (Figures 1 and 2), the water molecule is situated between the N−H of the amino group and the nitrogen of the five-membered ring. The **B + H_2O** complex of 4AT is predicted as more stable at all considered computational levels. The same result is obtained

TABLE 2: Relative Enthalpies ΔH_0 and Free Energies ΔG_{298} (kcal mol^{-1}) of Tautomers A and B for Compounds 2AT and 4AT Calculated at MP2/6-31+G(d,p), MP4/6-31+G(d,p)//MP2/6-31+G(d,p), and PCM/MP2/6-31+G(d,p)//MP2/6-31+G(d,p) Levels

	ΔH_0 (ΔG_{298})			
	2AT		4AT	
compound	A	B	A	B
		Isolated		
MP2/6-31+G(d,p)	0.00 (0.00)	0.00 (0.25)	1.33 (1.22)	0.00 (0.00)
MP4/6-31+G(d,p)	0.00 (0.00)	1.27 (1.50)	0.16 (0.05)	0.00 (0.00)
PCM/MP2/6-31+G(d,p)	2.61 (2.39)	0.00 (0.00)	4.43 (4.31)	0.00 (0.00)
		Monohydrated		
MP2/6-31+G(d,p)	0.94 (0.67)	0.00 (0.00)	1.94 (1.51)	0.00 (0.00)
MP4/6-31+G(d,p)	0.00 (0.00)	0.08 (0.34)	1.04 (0.60)	0.00 (0.00)
PCM/MP2/6-31+G(d,p)	2.58 (2.32)	0.00 (0.00)	3.95 (3.56)	0.00 (0.00)
		Trihydrated		
MP2/6-31+G(d,p)	3.64 (3.33)	0.00 (0.00)	4.92 (4.96)	0.00 (0.00)
MP4/6-31+G(d,p)	2.76 (2.44)	0.00 (0.00)	4.21 (4.25)	0.00 (0.00)
PCM/MP2/6-31+G(d,p)	3.86 (3.57)	0.00 (0.00)	6.15 (6.18)	0.00 (0.00)

TABLE 3: Interatomic Distances (Å) for Isolated and Trihydrated Tautomers A and B of 2AT and 4AT and Their Transition States (TS) with Available X-ray Data[14] Are Given in Parentheses

	B		TS		A	
distances	isolated	solvated	isolated	solvated	isolated	solvated
			2AT			
S1−C5	1.8047 (1.7953)	1.8047	1.8310	1.8080	1.8172	1.8135
S1−C2	1.7757 (1.7509)	1.7813	1.7345	1.7819	1.7809	1.7852
C2−N3	1.3034 (1.3333)	1.3203	1.3567	1.3550	1.3920	1.3835
N3−C4	1.3981 (1.3642)	1.3864	1.3745	1.3775	1.3751	1.3748
C5−C4	1.5476 (1.5206)	1.5420	1.5499	1.5342	1.5240	1.5252
C2−N7	1.3510 (1.3667)	1.3268	1.3098	1.3031	1.2785	1.2835
C4−O6	1.2222 (1.2329)	1.2273	1.2250	1.2289	1.2252	1.2265
N7−H8	1.0069	1.0137	1.0115	1.0180	1.0187	1.0207
N7−H14	1.0091	1.0250	1.3604	1.2869		1.8424
C5−H9	1.0880	1.0884	1.0885	1.0887	1.0884	1.0887
C5−H10	1.0881	1.0880	1.0885	1.0881	1.0884	1.0882
N3−H11		1.8714	1.3456	1.2981	1.0128	1.0338
O18−H8		1.9431		2.0024		2.0389
O15−H11				1.1878		1.7932
O12−H17				1.2384		1.7900
O15−H17		1.7813		1.1708		
O12−H14		1.8560		1.1975		
			4AT			
S1−C5	1.8005	1.8020	1.8258	1.8083	1.8203	1.8158
S1−C2	1.8269	1.8198	1.8349	1.8048	1.7882	1.7926
N3−C2	1.4071	1.3959	1.3848	1.3901	1.3861	1.3857
N3−C4	1.2986	1.3144	1.3463	1.3452	1.3862	1.3760
C4−C5	1.5159	1.5186	1.4950	1.5182	1.5185	1.5180
C2−O6	1.2133	1.2183	1.2146	1.2187	1.2188	1.2196
C4−N7	1.3533	1.3306	1.3112	1.3062	1.2820	1.2885
N7−H8	1.0064	1.0126	1.0126	1.0170	1.0196	1.0204
C5−H9	1.0902	1.0894	1.0887	1.0886	1.0882	1.0905
C5−H10	1.0909	1.0897	1.0904	1.0893	1.0901	1.0871
N7−H14	1.0091	1.0236	1.3664	1.2255		1.8349
N3−H11		1.8760	1.3456	1.2376	1.0130	1.0332
O18−H8		1.9772		2.0242		2.1372
O15−H11				1.2473		1.7959
O12−H17				1.2562		1.7988
O12−H14		1.8712		1.2602		
O15−H17		1.7794		1.1572		

TABLE 4: Calculated Energy Barriers $\Delta H_0^{\#}$ and $\Delta G_{298}^{\#}$ (in kcal mol^{-1}) for 2AT, 4AT, and Their Water Complexes. Imaginary Frequencies $\nu^{\#}$ Are in cm^{-1}. The Rate Constants Are in s^{-1}

	reaction											
	A → B				A + 1H$_2$O → *B* + 1H$_2$O				A + 3H$_2$O → *B* + 3H$_2$O			
computational level	$\Delta H_0^{\#}$	$\Delta G_{298}^{\#}$	k	$\nu^{\#}$	$\Delta H_0^{\#}$	$\Delta G_{298}^{\#}$	k	$\nu^{\#}$	$\Delta H_0^{\#}$	$\Delta G_{298}^{\#}$	k	$\nu^{\#}$
					2AT							
MP2/6-31+G(d,p)	45.17	44.91	7.4×10^{-21}	1935*i*	15.38	16.38	6.1×10^{-1}	1639*i*	13.63	15.36	3.4×10^{1}	1529*i*
MP4/6-31+G(d,p)//MP2/6-31+G(d,p)	49.54	49.29	4.6×10^{-24}		18.91	20.17	1.0×10^{-2}		17.82	19.54	2.9×10^{-2}	
PCM/MP2/6-31+G(d,p)	49.25	49.05	6.8×10^{-24}		17.29	18.50	1.7×10^{-1}		14.34	16.32	6.8	
					4AT							
MP2/6-31+G(d,p)	47.15	47.14	1.7×10^{-22}	1942*i*	16.33	17.29	1.3×10^{1}	1649*i*	14.29	15.85	1.5×10^{1}	1506*i*
MP4/6-31+G(d,p)//MP2/6-31+G(d,p)	50.33	50.32	8.0×10^{-25}		19.84	20.79	3.6×10^{-3}		18.31	19.87	1.7×10^{-2}	
PCM/MP2/6-31+G(d,p)	51.89	52.11	3.9×10^{-26}		18.51	19.68	2.3×10^{-2}		15.78	17.62	7.5×10^{-1}	

for the monohydrated complex of 2AT at MP2/6-31+G(d,p) and PCM/MP2/6-31+G(d,p)//MP2/6-31+G(d,p) levels. However, the inclusion of correlation effects of high order, MP4/6-31+G(d,p)//MP2/6-31+G(d,p) predict **A** + **H_2O** as more stable (Table 2).

Considering the trihydrated complexes of 2AT and 4AT (Figures 3 and 4), we assume that two of the water molecules are situated between the N−H of the amino group and the nitrogen of the five-membered ring, while the third water molecule is bonded to the N−H of the same amino group. The values of the relative enthalpies and free energies calculated at MP2 and MP4 levels for the trihydrated complexes (Table 2) indicate that the **B** + **3H_2O** complex is more stable. According to the obtained results the differences in the stabilities of the trihydrated complexes of tautomers **A** and **B** of 2AT and 4AT increase significantly relative to the monohydrated ones.

The MP2/6-31+G(d,p) optimized geometries of the trihydrated complexes of tautomers **A** and **B** are presented in Figures 3 and 4. Selected interatomic distances are collected in Table 3. The obtained ab initio results for the geometry of tautomer **B** of 2AT are in agreement with the available X-ray data.[14]

As expected, formation of a trihydrated complex induces changes in the geometrical parameters of **A** and **B** mainly in the region of intermolecular hydrogen bonding. According to calculations at MP2/6-31+G(d,p) level for tautomer **B** of 2AT, the changes in the N−H and C−N bonds are strongest. The formation of an intermolecular hydrogen bond in the **B** + **3H_2O** complex leads to a lengthening of the N7−H8 and N7−H14

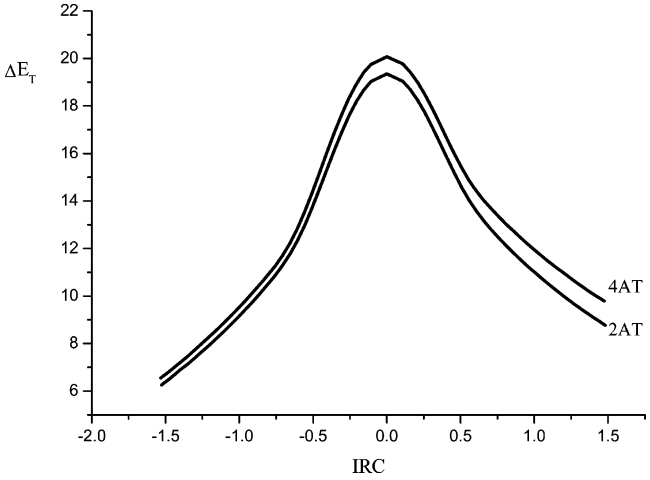

Figure 5. MP2/6-31+G(d,p) calculated IRC profiles of the solvent-mediated proton-transfer reactions in the trihydrated 2AT (Figure 3) and trihydrated 4AT (Figure 4). ΔE_T is in kcal mol^{-1} and IRC in amu$^{1/2}$bohr.

bonds by 0.0068 and 0.0159 Å, respectively. The lengthening of the C2−N3 bond is more strongly expressed (+0.0169 Å) than the shortening of the N3−C4 bond (−0.0117 Å) (Table 3). Similar changes are observed in tautomer **B** of 4AT. The N3−C4 bond lengthens by 0.0158 Å while the C2−N3 bond shortens by 0.0112 Å. The N7−H8 and N7−H14 bonds lengthen by 0.0062 and 0.0145 Å, respectively. The exocyclic C−N bond also shortens strongly: −0.0242 Å for 2AT and −0.0227 Å for 4AT.

The formation of an intermolecular hydrogen bond in the **A** + **3H$_2$O** complex leads to a lengthening of the N3−H11 bond by 0.0210 Å while the N3−C4 bond almost does not change. The N7−H8 and N7−C2 bonds also lengthen because of intermolecular hydrogen bonding by 0.0020 and 0.0050 Å, respectively. The N3−C2 bond shortens by 0.0085 Å in comparison with the isolated molecule **A**. Some differences are observed in the geometrical parameters of tautomer **A** of 4AT. Including of three water molecules leads to lengthening of the N3−H11 and C2−S1 bonds by 0.0202 and 0.0044 Å, respectively. For tautomer **A** of 4AT the MP2/6-31+G(d,p)-calculated N3−C4 and S1−C5 bonds lengths shorten by 0.0102 and 0.0045 Å, respectively, while in 2AT these bonds do not change.

It should be noted that the water molecules in the trihydrated complexes of 2-aminothiazolidine-4-one and 4-aminothiazolidine-2-one lie in the plane of the molecule.

4.2. Monoassisted or "Relay" Proton Transfer? In our opinion, a 42 kcal mol^{-1} proton transfer barrier height is unobservable by modern experimental techniques because the calculated rate constant for the prototypic molecule is only 1.0 × 10^{-21} s^{-1}. In contrast, a calculated barrier height of less than 20 kcal mol^{-1} can be regarded as observable because the rate constant is greater than 1.0 × 10^{-4} s^{-1}.[28]

In this study, we calculated the values of proton transfer barriers between the studied isolated and corresponding monohydrated and trihydrated tautomers of 2AT and 4AT. We consider two different reaction mechanisms of tautomerisation in monohydrated and trihydrated complexes. In the first case (Figures 1 and 2), only one water molecule assists the proton transfer from the amino group to the nitrogen atom in the five-membered ring—monoassisted proton transfer. In the second case, (Figures 3 and 4), a hydrogen atom from the amino group migrates to the water molecule, a proton from this molecule migrates to a second water molecule and a proton from the second water molecule migrates to the nitrogen atom in the ring—"relay" proton transfer.

The transition state structures corresponding to the direct and water-assisted proton transfer reactions were located. The predicted TS were verified by establishing that the Hessians have only one negative eigenvalue. The calculated barriers of the tautomerisation reactions for the isolated (**B** → **A**), mono- and trihydrated 2AT and 4AT, and the respective imaginary frequencies, calculated at the MP2/6-31+G(d,p) level of theory, are presented in Table 4. The inclusion of high-order correlation contributions increases the barrier heights. Because of the sensitivity of the barrier height to the employed level of electron correlation[28] the observed differences between the MP4 and MP2 results are not surprising.

Simple transition state theory using the Eyring equation was applied to estimate the rate constants k of the **B** → **A** process. The computed proton-transfer rate constants k are listed in Table 4. According to the rate constant values obtained at all levels of calculation, "relay" proton transfer can occur ($k_{\text{relay PT}} = 10^{1}-10^{-2} \gg k_{\text{direct PT}} = 10^{-21}-10^{-26}$), although slowly. The activation energy of the tautomerisation reaction **B** → **A** via direct

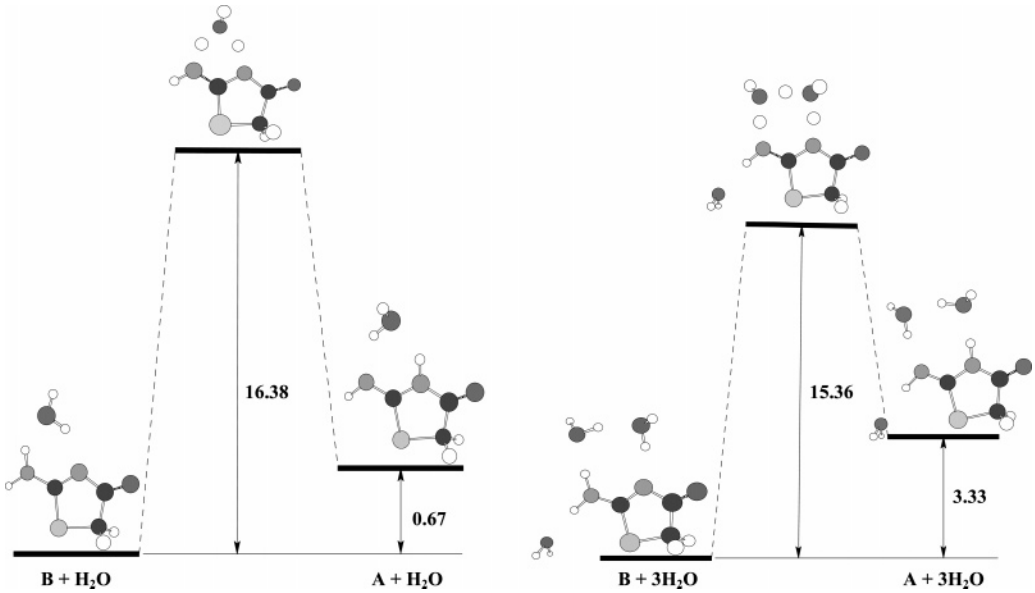

Figure 6. Energy profile of the tautomerization reactions **B** + **H$_2$O** → **A** + **H$_2$O** and **B** + **3H$_2$O** → **A** + **3H$_2$O** of 2AT, calculated at the MP2/6-31+G(d,p) level. The free energies ΔG_{298} and activation barriers are given in kcal mol^{-1}.

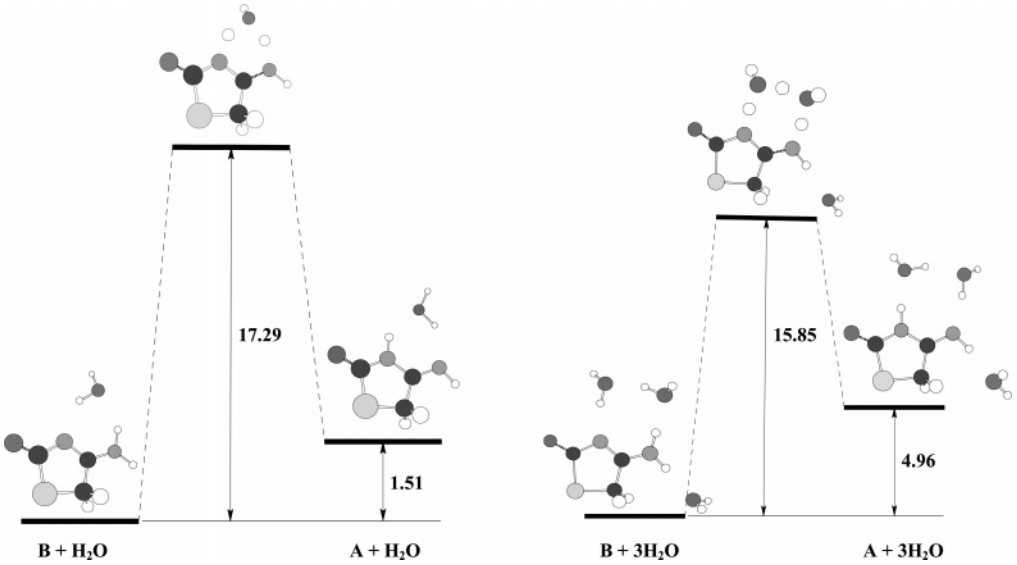

Figure 7. Energy profile of the tautomerization reactions **B** + **H$_2$O** → **A** + **H$_2$O** and **B** + **3H$_2$O** → **A** + **3H$_2$O** of 4AT, calculated at the MP2/6-31+G(d,p) level. The free energies ΔG_{298} and activation barriers are given in kcal mol^{-1}.

TABLE 5: Selected Intermolecilar Distances (Å) and Bond Angles (deg) in the Hydrated Complexes of 2AT and 4AT Shown in Figures 1−4

	A + H_2O			B + H_2O	
parameter	2AT	4AT	parameter	2AT	4AT
N7−H14	2.017	2.012	H14−O12	1.970	1.977
H11−O12	1.947	1.959	N3−H11	2.010	2.018
N7−O12	2.845	2.841	N7−O12	2.858	2.859
N3−O12	2.829	2.827	N3−O12	2.835	2.836
N7−H14−O12	141.3	141.4	N7−H14−O12	144.1	143.3
N3−H11−O12	142.6	140.8	N3−H11−O12	140.8	139.9
	A + $3H_2O$			B + $3H_2O$	
parameter	2AT	4AT	parameter	2AT	4AT
N7−H14	1.842	1.835	H14−O12	1.856	1.871
H11−O15	1.793	1.796	N3−H11	1.871	1.876
N7−O12	2.822	2.816	N7−O12	2.879	2.893
N3−O15	2.824	2.826	N3−O15	2.840	2.843
N7−H14−O12	171.3	171.4	N7−H14−O12	175.7	175.4
N3−H11−O15	174.9	174.1	N3−H11−O15	167.6	166.8

intramolecular proton transfer is very high and the tautomerisation process should not occur. Inclusion of water molecules strongly reduces the activation energy. For the trihydrated complex, the proton-transfer activation energy is lower than that for the isolated molecule by 28.65−29.75 kcal mol^{-1} for 2AT and 30.45−32.49 kcal mol^{-1} for 4AT at different computational levels. The potential energies of the trihydrated complexes of 2AT and 4AT along the minimum energy path, calculated at MP2/6-31+G(d,p) level are illustrated in Figure 5. The **B** → **A** reaction for 2AT has a lower barrier than that for 4AT.

The differences in the energy barriers for the monowater assisted proton-transfer reaction are higher than for the "relay" PT by 1.02 and 1.44 kcal mol^{-1} for 2AT and 4AT, respectively (Figures 6 and 7). Thus, the participation of two water molecules in a proton transfer reaction should be more favorable than the participation of only one water molecule. A possible explanation could be given on the base of comparison of the intermolecular hydrogen bonds and respective bond angles in the reaction site of the solute−solvent cluster (Figures 1−4, Table 5). On the basis of the calculated geometrical parameters of mono- and trihydrated tautomers of 2AT and 4AT, the predicted intermolecular hydrogen bonds for these systems are moderately strong. The N7−H14−O12 and N3−H11−O12 bond angles in the monohydrated complex of 2AT are in the 140.8−144.1° region. In the trihydrated complex these become near-linear: 167.6−175.7°. In addition, the proton displacements (distance between the initial and end position of the proton) d_{H14} and d_{H11} in monohydrated 2AT are 1.1531 and 1.1394 Å, respectively, while in the trihydrated complex they are shorter—d_{H14} = 0.9081 Å and d_{H11} = 0.9216 Å (Figures 1 and 3). The proton displacement d_{H11} = 1.1586 Å in monohydrated 4AT shortens to 0.9356 Å in the trihydrated complex, while the d_{H14} values are 1.2147 and 1.3736 Å for the mono- and trihydrated complexes, respectively (Figures 2 and 4).

In the monohydrated complexes of 2AT and 4AT, there is no charge transfer from 2AT (4AT) to the water molecule (Figures 1 and 2). The analysis of the transition state geometries

TABLE 6: GIAO ^{13}C Chemical Shifts (ppm) Calculated at Hartree−Fock (HF) and DFT Level, Where the Geometry Is Optimized at the MP2/6-31+G(d,p) Level. Chemical Shifts Not Including the Solvent Effects Are Given in Parentheses

carbon atoms	exptl.	HF/6-31+G(d,p)	B3LYP/6-31+G(d,p)
		2AT	
C2	182.7[a]	196.8 *(191.7)*	184.7 *(180.6)*
C4	187.7[a]	194.7 *(188.8)*	187.3 *(182.2)*
C5	39.8[a]	38.4 *(38.2)*	46.3 *(46.3)*
		2AT + H_2O	
C2	195.0[b]	196.8 *(192.9)*	184.4 *(181.1)*
C4	195.0[b]	193.4 *(188.0)*	185.9 *(181.1)*
C5	43.1[b]	37.4 *(36.9)*	44.8 *(44.4)*
		2AT + $3H_2O$	
C2	195.0[b]	194.2 *(190.4)*	182.5 *(179.0)*
C4	195.0[b]	194.1 *(189.2)*	186.0 *(181.6)*
C5	43.1[b]	36.5 *(35.7)*	43.6 *(42.9)*
		4AT	
C2	184.3[a]	194.7 *(186.9)*	187.7 *(181.3)*
C4	181.9[a]	189.6 *(184.9)*	177.8 *(173.6)*
C5	37.5[a]	32.6 *(31.0)*	41.2 *(39.5)*
		4AT + H_2O	
C2	190.8[c]	193.7 *(186.7)*	186.5 *(180.7)*
C4	183.8[c]	189.3 *(185.6)*	177.1 *(173.6)*
C5	38.6[c]	32.6 *(31.1)*	41.3 *(39.7)*
		4AT + $3H_2O$	
C2	190.8[c]	194.6 *(188.5)*	186.8 *(181.7)*
C4	183.8[c]	187.7 *(184.8)*	175.9 *(173.1)*
C5	38.6[c]	33.0 *(31.8)*	41.9 *(40.7)*

[a] Solvent DMSO-d_6. [b] Solvent D_2O. [c] Solvent D_2O/CD_3OD.

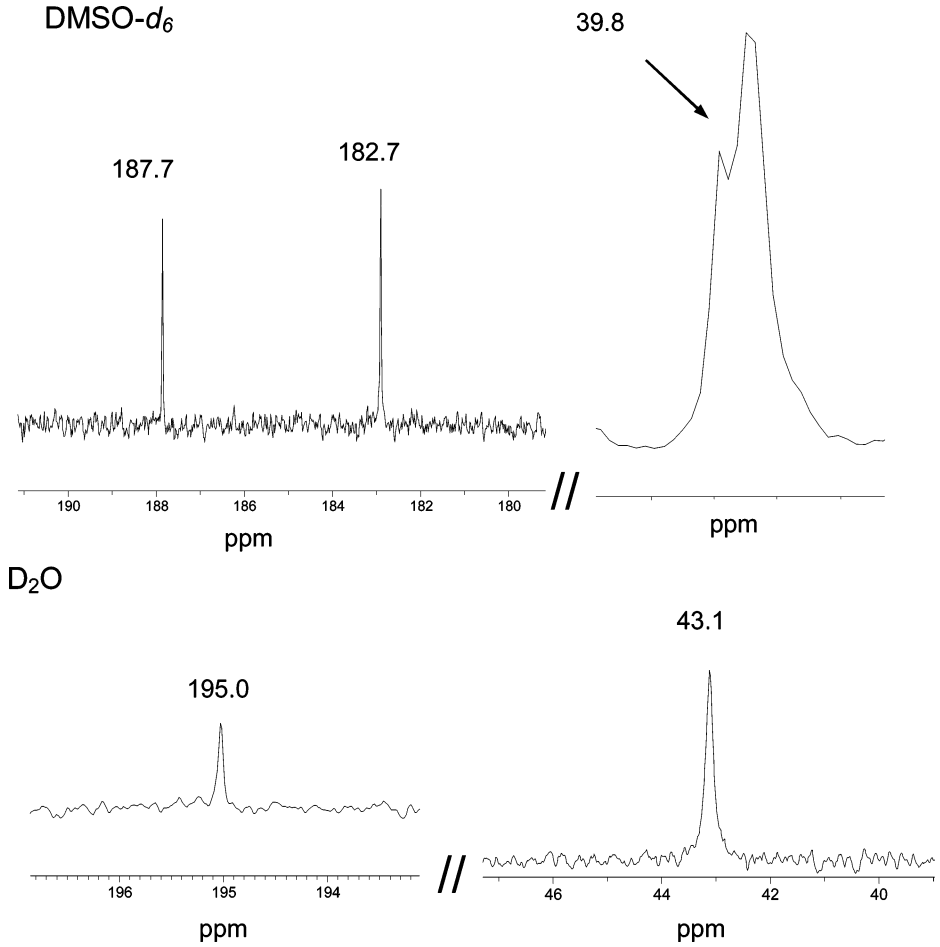

Figure 8. ^{13}C NMR spectra of 2AT in solvents DMSO-d_6 and D_2O.

of the monohydrated complexes of 2AT and 4AT reveal that H14 attached to the N7 atom of 2AT or 4AT migrates toward the water molecule and H11 attached to the O12 migrates to the N3 atom. The distances O12−H13, O12−H14, and O12−H11 in **TS** + $\mathbf{H_2O}$ in 2AT are 0.967, 1.199, and 1.198 Å, respectively, while N7−H14 and N3−H11 are 1.303 and 1.302 Å, respectively. In **TS** + $\mathbf{H_2O}$ of its isomer, 4AT, the interatomic distances are as follows: O12−H13, 0.967 Å; O12−H11, 1.208 Å; O12−H14, 1.198 Å; N7−H14, 1.302 Å; N3−H11, 1.292 Å.

In the case of trihydrated complexes, **A** + $\mathbf{3H_2O}$ and **B** + $\mathbf{3H_2O}$, the water molecules situated between the exocyclic nitrogen atom and the nitrogen of the five-membered ring are hydrogen bonded with each other (Figures 3 and 4). According to the Mulliken population analysis of 2AT (Figure 3), the water molecule hydrogen bonding with H8 has 0.011 e^- of negative charge while water dimer has practically no negative charge (−0.002 e^-). A more pronounced result was obtained for the trihydrated complexes of 4AT (Figure 4): −0.006 e^- for water dimer and −0.016 e^- for the third water molecule. In the transition state, **TS**+$\mathbf{3H_2O}$ of both compounds the proton H17 is shared by both water molecules (Table 3). The migrating protons H11 and H14 are situated more closely to oxygen atoms of the water cluster in the case of 2AT while in the **TS**+$\mathbf{3H_2O}$ of 4AT they are shared by the oxygen atoms of the water cluster and the nitrogen atoms of 4-aminothiazolidine-2-one.

Thus, the transition state geometries are of zwitterionic type having a $H_3O^+\cdots$2AT(4AT)$^-$ type of structure for the monohydrated forms, and a $H_5O_2^+\cdots(2AT+H_2O)^-$ and $H_5O_2^+\cdots(4AT+H_2O)^-$ type of structure for the trihydrated forms. The Mulliken population analysis shows that for the monohydrated transition structure, the H_3O^+ ion has 0.566 (0.557) e^- of positive charge while the same amount of negative charge is found at the 2AT (4AT) anion at MP2/6-31G(d,p) level of theory. In the case of the trihydrated transition structure, the $H_5O_2^+$ ion has 0.614 and 0.517 e^- of positive charge for $H_5O_2^+\cdots(2AT+H_2O)^-$ and $H_5O_2^+\cdots(4AT+H_2O)^-$, respectively. The 2AT and 4AT anions have 0.605 and 0.501 e^- of negative charge while the third water molecule does not change its negative charge in the transition structure compared to the **A** + $\mathbf{3H_2O}$ and **B** + $\mathbf{3H_2O}$ complexes. Thus, a charge analysis of the hydrated transition structures shows that the zwitterionic nature is more pronounced in the trihydrated form compared to the monohydrated form. Our results correspond to these reported by Shukla and Leszczynski[29,30] for hydrated complexes of hypoxanthine.

If we consider the trihydrated complexes of 2AT and 4AT as embedded in a continuum reaction field, the activation enthalpies ($\Delta H_0^{\#}$) calculated at MP2/6-31+G(d,p) level increase by 0.71 and 1.49 kcal mol^{-1}, respectively (Table 4) relative to the gas-phase cluster. The free activation energies ($\Delta G_{298}^{\#}$) also increase: by 0.96 kcal mol^{-1} for 2AT and by 1.77 kcal mol^{-1} for 4AT.

4.3. Are Different Tautomeric Forms of 2AT and of 4AT Identified by NMR and UV Spectroscopy? The PCM/MP2/6-31+G(d,p) calculated Gibbs free energy differences for **A** and **B** in water are presented in Table 2. In all cases tautomer **B** is preferred. The differences in the Gibbs free energies for trihydrated 2AT and 4AT are 3.57 and 6.18 kcal mol^{-1}, respectively. On the basis of these differences, the percent concentration of tautomer **A** was calculated to be 0.24% for 2AT and 0.003% for 4AT.

To study the behavior of structures **A** and **B** in solution, ^{1}H and ^{13}C NMR spectra were recorded in solvents DMSO-d_6 and D_2O for 2AT and in DMSO-d_6 and D_2O/CD_3OD for 4AT because of the low solubility of the latter in water. The HF/6-31+G(d,p) and B3LYP/6-31+G(d,p) calculated^{13}C chemical shifts of tautomer **B** in these solvents (DMSO in the case of isolated species and water in the case of the complexes) were compared to the experimentally observed values (Table 6). In our previous paper,[1] we showed that the signals of tautomers **A** are inconsistent with the experimentally observed values, as the MP2/6-311+G(d,p) calculated ^{13}C chemical shifts for tautomer **A** of 4AT are as follows: C2, 170.2 ppm; C4, 162.4 ppm; C5, 37.5 ppm. We assume that because of the very low concentration of tautomer **A** its signals cannot observed in the NMR spectra of 2AT and 4AT in D_2O and D_2O/CD_3OD, respectively.

The chemical shifts of 2AT calculated at HF level without taking into account the solvent effect are closer to the experimental data for isolated molecules, while including of the solvent as a dielectric results in reliable ^{13}C NMR spectrum prediction for the water complexes. For the B3LYP calculated chemical shifts the situation is different. There is good agreement between the experimental and B3LYP-calculated chemical shifts with inclusion of solvent effects for the isolated tautomer **B**, and unreliable prediction of chemical shifts for the hydrated complexes, both with and without inclusion of the solvent effect. For the trihydrated complex of 2AT the most noticeable agreement between calculated and experimental chemical shifts is for HF-calculated chemical shifts including solvent effect, where the values for C2 and C4 are predicted accurately ($\Delta\delta$ = 0.8 and 0.9 ppm respectively). The ^{13}C NMR spectra of 2AT in DMSO-d_6 and D_2O are presented in Figure 8. In the spectrum in DMSO-d_6 signals for C2 (182.7 ppm) and C4 (187.7 ppm) are observed, while in D_2O we observe only one signal (195.0 ppm). The coincidence of the signals for C2 and C4 is well predicted by the HF calculations for the chemical shifts of these carbon atoms in the respective solvents, especially with taking into account the solvent effect in the case of the trihydrated complex.

The chemical shifts of 4AT, calculated at HF level without taking into account the solvent effect, are closer to the experimental data for isolated molecules. The inclusion of the solvent as dielectric does not improve the spectrum prediction for the water complexes. The B3LYP calculated chemical shifts are also not well predicted, as the calculations with inclusion of the solvent effects are in better agreement relative to these without solvent effects.

As we noted above because of the very low concentration of tautomer **A** its signals cannot be observed in the ^{13}C NMR spectra of 2AT and 4AT in water. In this case UV spectroscopy should be useful. The absorption spectra of 2AT and 4AT in water are presented in Figure 9. The UV−vis absorption spectrum of 2AT consists of two bands. The more intensive band (ϵ = 25 200 cm^{-1} M^{-1}) is located at 214 nm and that with lower intensity (ϵ = 10 000 cm^{-1} M^{-1}) at 251 nm. The absorption spectrum of its isomer, 4AT, has also two bands − at 212 nm (ϵ = 8104 cm^{-1} M^{-1}) and 253 nm (ϵ = 3268 cm^{-1} M^{-1}) but with lower intensity.

TD DFT B3LYP/aug-cc-pVTZ calculations were performed to predict the absorption maxima of tautomers **A** and **B** of 2AT and 4AT. For tautomer **B** of 2AT, two intensive absorption maxima were calculated at 247 and 217 nm. The computed vertical singlet transition energies were found to be in good agreement with the corresponding experimental data. For tautomer **A** absorption maxima were predicted at 227 and 205 nm (Figure 9). They also fall in the range of the absorption maximum of tautomer **B**. Similar results were also found for 4AT (Figure 9). Three intensive absorption maxima were calculated for tautomer **B** at 259, 210, and 207 nm, and for tautomer **A** at 234, 225, and 204 nm.

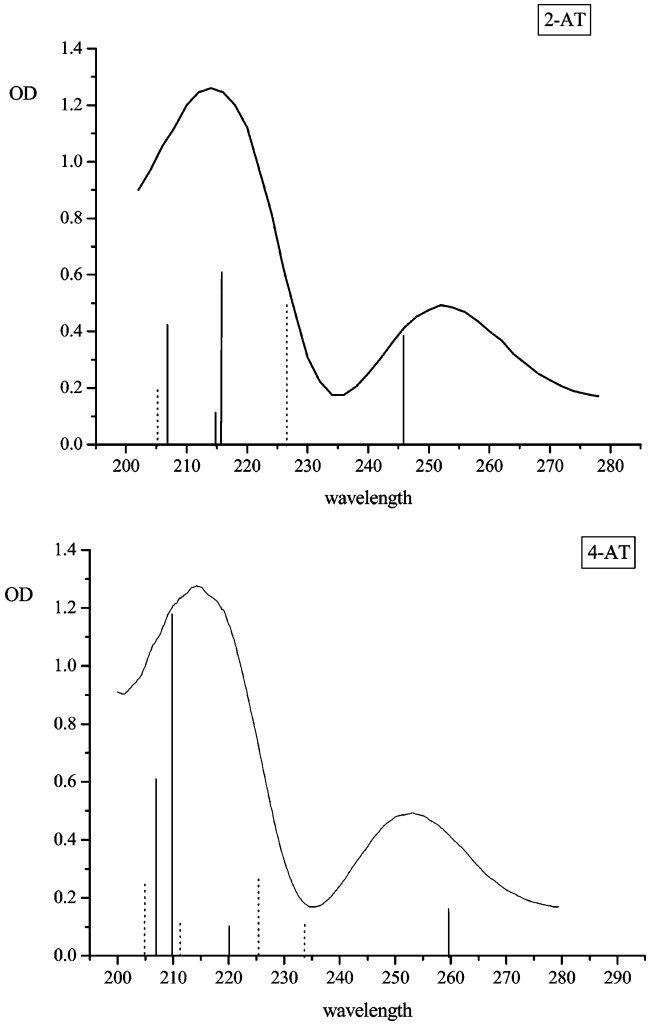

Figure 9. UV absorption spectra of 2AT and 4AT in water. Optical density (OD) is in arbitrary units and wavelength in nm. TD DFT B3LYP/aug-cc-pVTZ calculated π-π* electron transitions for tautomer **B** (solid line) and tautomer **A** (dot line).

This would explain why it is impossible to detect experimentally the existence of tautomer **A**.

5. Conclusions

The paper studies the solvation of 2-aminothiazolidine-4-one and 4-aminothiazolidine-2-one using a quantum-chemical approach. The effects of the water as solvent are introduced at three different levels—through a continuum description, using solute−solvent clusters (one or three water molecules) and using the same clusters embedded in an external continuum. We show that when a water dimer is located in the reaction site between the hydrogen atom from the amino group and the nitrogen atom in the ring, the assistive effect ("relay" proton transfer) of the water molecules is strengthened. In this case, the intermolecular hydrogen bonds in the solute−solvent clusters become near-linear and the proton travels smaller distances than in the case of monoassisted proton transfer.

To confirm the reliability of our considerations, NMR calculations were performed in the framework of the three

different solvation models: a continuum only description, a discrete description in terms of solute−solvent clusters, and a discrete/continuum description in terms of clusters embedded in a continuum. The results obtained by the latter model are in best agreement with the experimental ones.

Acknowledgment. The authors are indebted to Mr. Sasho Chorbadjiev, Faculty of Chemistry, Sofia University, for the synthesis of 2-aminothiazolidine-4-one and 4-aminothiazolidine-2-one and to Dr Pavlina Dolashka and Dr. Irina Petkova, Institute of Organic Chemistry, Bulgarian Academy of Sciences, for measuring the UV spectra. We are grateful to Dr Benoit Champagne, Notre-Dame de la Paix University, Namur, Belgium, for help with computing facilities.

References and Notes

(1) Angelova, S.; Enchev, V.; Markova, N.; Denkova, P.; Kostova, K. *J. Mol. Struct. THEOCHEM* **2004**, *711*, 201−207.

(2) Brown, F. C. *Chem. Rev.* **1961**, *61*, 463−521.

(3) Comrie, A. M. *J. Chem. Soc.* **1964**, 3748−3480.

(4) Akerblom, E. *Acta Chem. Scand.* **1967**, *21*, 1437.

(5) Khovratovich, N. N.; Chizhevskaya, I. I. *Khim. Geterocycl. Soed.* **1967**, 637−641.

(6) Pereseleni, E. M.; Sheinker, Yu. N.; Zosimova, N. P. *Zh. Fiz. Khim.* **1965**, *39*, 926−931.

(7) Amirthalingam, V.; Muralidharan K. V. *Acta Crystallogr.* **1972**, *28B*, 2421−2423.

(8) Durden, J. A.; Stasbury, H. A.; Catlette, W.H. *J. Am. Chem. Soc.* **1959**, *81*, 1943−1946.

(9) Najer, H.; Giudicelli, R.; Morel, C.; Menin, J. *Bull. Chem. Soc. Fr.* **1963**, 1022−1026.

(10) Ramsh, S. M.; Ginak, A. I.; Smorigo, N. A.; Basova, Yu. G.; Sochilin, E. G. *Zh. Org. Khim.* **1978**, *14*, 1327−1332.

(11) Ramsh, S. M.; Smorigo, N. A.; Ginak, A. I. *Khim. Geterocycl. Soed.* **1984**, 1066−1070.

(12) Ramsh, S. M.; Smorigo, N. A.; Khrabrova, E. S. *Khim. Geterocycl. Soed.* **1985**, 32−37.

(13) Valls, N.; Segarra, V. M.; Alcalde, E.; Marin, A.; Elguero, J. *J. Prakt. Chem.* **1985**, *327*, 251−260.

(14) Steel, R. J.; Guard, J. A. M. *Acta Crystallogr.* C **1994**, *50*, 1721−1723.

(15) Schmidt, M. W.; Gordon, M. S.; Dupuis, M. *J. Am. Chem. Soc.* **1985**, *107*, 2585−2589.

(16) Baldridge, K. K.; Gordon, M. S.; Steckler, R.; Truhlar, D. G. *J. Phys. Chem.* **1989**, *93*, 5107−5119.

(17) Granovsky, A. A. www http://classic.chem.msu.su/gran/gamess/index.html.

(18) Schmidt, M. W.; Baldridge, K. K.; Boatz, J. A.; Elbert, S. T.; Gordon, M. S.; Jensen, J. H.; Koseki, S.; Matsunaga, N.; Nguyen, K. A.; Su, S.; Windus, T. L.; Dupuis, M.; Montgomery, J. A. *J. Comput. Chem.* **1993**, *14*, 1347−1363.

(19) Miertus, S.; Scrocco, E.; Tomasi, J. *Chem. Phys.* **1981**, *55*, 117−129.

(20) Miertus, S.; Tomasi, J. *Chem. Phys.* **1982**, *65*, 239−245.

(21) Frisch, M. J.; Trucks, G. W.; Schlegel, H. B.; Scuseria, G. E.; Robb, M. A.; Cheeseman, J. R.; Zakrzewski, V. G.; Montgomery, J. A. Jr.; Stratmann, R. E.; Burant, J. C.; Dapprich, S.; Millam, J. M.; Daniels, A. D.; Kudin, K. N.; Strain, M. C.; Farkas, O.; Tomasi, J.; Barone, J.; Cossi, M.; Cammi, R.; Mennucci, B.; Pomelli, C.; Adamo, C.; Clifford, S.; Ochterski, J.; Petersson, G. A.; Ayala, P. Y.; Cui, Q.; Morokuma, K.; Malick, D. K.; Rabuck, A. D.; Raghavachari, K.; Foresman, J. B.; Cioslowski, J.; Ortiz, J. V.; Baboul, A. G.; Stefanov, B. B.; Liu, G.; Liashenko, A.; Piskorz, P.; Komaromi, I.; Gomperts, R.; Martin, R. L.; Fox, D. J.; Keith, T.; Al-Laham, M. A.; Peng, C. Y.; Nanayakkara, A.; Gonzalez, C.; Challacombe, M.; Gill, P. M. W.; Johnson, B.; Chen, W.; Wong, M. W.; Andres, J. L.; Gonzalez, C.; Head-Gordon, M.; Replogle, E. S.; Pople, J. A. *Gaussian 98*, revision A.7, Gaussian, Inc.: Pittsburgh, PA, 1998.

(22) Ditchfield, R. *Mol. Phys.* **1974**, *27*, 789−807.

(23) Wolinski, K.; Hinton, J. F.; Pulay, P. *J. Am. Chem. Soc.* **1990**, *112*, 8251−8260.

(24) Frisch, M. J.; Trucks, G. W.; Schlegel, H. B.; Scuseria, G. E.; Robb, M. A.; Cheeseman, J. R.; Montgomery, J. A., Jr.; Vreven, T.; Kudin, K. N.; Burant, J. C.; Millam, J. M.; Iyengar, S. S.; Tomasi, J.; Barone, V.; Mennucci, B.; Cossi, M.; Scalmani, G.; Rega, N.; Petersson, G. A.; Nakatsuji, H.; Hada, M.; Ehara, M.; Toyota, K.; Fukuda, R.; Hasegawa, J.; Ishida, M.; Nakajima, T.; Honda, Y.; Kitao, O.; Nakai, H.; Klene, M.; Li, X.; Knox, J. E.; Hratchian, H. P.; Cross, J. B.; Adamo, C.; Jaramillo, J.; Gomperts, R.; Stratmann, R. E.; Yazyev, O.; Austin, A. J.; Cammi, R.; Pomelli, C.; Ochterski, J. W.; Ayala, P. Y.; Morokuma, K.; Voth, G. A.; Salvador, P.; Dannenberg, J. J.; Zakrzewski, V. G.; Dapprich, S.; Daniels, A. D.; Strain, M. C.; Farkas, O.; Malick, D. K.; Rabuck, A. D.; Raghavachari, K.; Foresman, J. B.; Ortiz, J. V.; Cui, Q.; Baboul, A. G.; Clifford, S.; Cioslowski, J.; Stefanov, B. B.; Liu, G.; Liashenko, A.; Piskorz, P.; Komaromi, I.; Martin, R. L.; Fox, D. J.; Keith, T.; Al-Laham, M. A.; Peng, C. Y.; Nanayakkara, A.; Challacombe, M.; Gill, P. M. W.; Johnson, B.; Chen, W.; Wong, M. W.; Gonzalez, C.; Pople, J. A. Gaussian 03, Revision B.04; Gaussian, Inc.: Pittsburgh, PA, 2003.

(25) Casida, M. E.; Jamorski, C.; Casida, K. C.; Salahub, D. R. *J. Chem. Phys.* **1998**, *108*, 4439−4449. Robb, M. A.; Garavelli, M.; Olivucci, M.; Bernardi, F. In *Reviews in Computational Chemistry*; Lipkowitz, K. B., Boyd, D. B. Eds.; Wiley-VCH: New York, 2000, Vol. 15, p 87.

(26) Davies, W.; Maclaren, J. A.; Wilkinson, L. R. *J. Chem. Soc.* **1950**, *3491*, 3491−3494.

(27) Komaritsa, I. O. *Khim. Geterocycl. Soedin.* **1968**, 436−437.

(28) Markova, N.; Enchev, V.; Timtcheva, I. *J. Phys. Chem. A* **2005**, *109*, 1981−1988.

(29) Shukla, M. K.; Leszczynski, J. *J. Phys. Chem. A* **2000**, *104*, 3021−3027.

(30) Shukla, M. K.; Leszczynski, J. *J. Mol. Struct. THEOCHEM* **2000**, *529*, 99−112.